DOI: https://doi.org/10.15625/0868-3166/22403

# Numerical investigation of droplet formation in T-junction microfluidic system with a semi-NACA-shaped squeezer

Ich Long Ngo<sup>1,‡</sup>, Van Nam Dao<sup>2</sup>, Thi Xuan Chu<sup>2,†</sup>

E-mail: †xuan.chuthi@hust.edu.vn; ‡long.ngoich@hust.edu.vn

Received 14 February 2025 Accepted for publication 9 July 2025 Published 11 July 2025

**Abstract.** We present a numerical investigation of droplet formation in a T-junction microfluidic system with a semi-NACA-shaped squeezer. A two-dimensional numerical model is employed to simulate the droplet formation process using the Volume of Fluid method. The integration of this semi-NACA squeezer positively affects the droplet formation dynamics under identical operating conditions. By varying the squeezer size, an inverse correlation is observed between squeezer size and droplet size. Additionally, the droplet formation process in the microfluidic T-junction device is highly dependent on the viscosity ratio, with droplet size decreasing as the viscosity ratio increases. These findings contribute to a better understanding of the droplet dynamics in T-junction devices, paving the way for new applications in microfluidic technology.

Keywords: microdroplet; T-junction microfluidic system; semi-NACA-shaped squeezer; volume of fluid.

Classification numbers: 47.55.db; 47.61.Jd; 47.11.Df.

# 1. Introduction

Droplet-based microfluidics has increasingly attracted the attention of researchers due to the immiscible nature of the two fluids and their scalability benefits. Various applications have been explored, including drug delivery [1], chemical synthesis [2], and food technology [3]. In these applications, precise control of microdroplets is crucial, drawing interest from both experimental and simulation researchers [4, 5]. Baroud *et al.* [6] investigated the influence of flow fields on droplet formation in different microfluidic systems, including co-flow injection devices,

<sup>&</sup>lt;sup>1</sup>School of Mechanical Engineering, HUST, No. 01, Dai Co Viet, Hai Ba Trung, Hanoi, Vietnam <sup>2</sup>School of Materials Science and Engineering, HUST, No. 01, Dai Co Viet, Hai Ba Trung, Hanoi, Vietnam

T-junctions, and flow-focusing devices. Loo *et al.* [7] experimentally demonstrated that droplet volume depends on both the capillary number and flow rate ratio in a cross-junction microchannel, with and without the addition of surfactants to the continuous phase. Different regimes, including slug, dripping, and jetting, have been observed in T-junction microfluidic systems [8, 9]. Ngo *et al.* [10] conducted numerical studies on a microfluidic cross-junction device and found that the viscosity ratio and the junction angle strongly influence droplet formation and size. Many researchers have also performed simulation studies on different flow regimes within T-junction microfluidic systems [11, 12]. Due to its simple fabrication and the ability to produce synchronized monodispersed droplets, the T-junction is one of the most widely employed passive techniques in droplet-based microfluidics.

The T-junction microfluidic design, one of the most commonly used structures, was first introduced by Thorsen in 2001 [13], where water droplets were generated via pressure-driven laminar flow in microchannels. Nisisako *et al.* [14] conducted experiments by adjusting the flow rates of the continuous and dispersed phases, demonstrating that the droplet size and production rate could be controlled by independently modifying these flow rates. In 2006, Garstecki *et al.* [11] experimentally identified three droplet formation regimes - squeezing, dripping, and jetting in T-junction devices. In 2008, Christopher *et al.* [15] focused on the transition between squeezing and dripping by altering viscous forces. To investigate droplet formation further, some researchers introduced obstacles into the channel. Wang *et al.* [16] showed that droplet formation is significantly affected when a venturi-shaped obstacle is placed on the upper wall of the T-junction. Nath and colleagues [17] used semicircular obstacles to study changes in droplet formation based on obstacle size and position.

Computational fluid dynamics (CFD) is widely used to study multiphase flows in microfluidic devices. Numerous numerical models and techniques have been developed in previous research. Liu and Zhang [18] used the Lattice Boltzmann method (LBM) to simulate multiphase flows in a cross-junction channel under low capillary number conditions. Similarly, Han *et al.* [19] applied the level set method (LSM) to investigate droplet formation in microfluidic flow-focusing devices (MFFDs), considering various influencing parameters. Sang *et al.* [20] utilized the volume-of-fluid (VOF) method to analyze the effects of viscosity on droplet formation. Each method has its own advantages and disadvantages depending on the research purpose. LBM offers a simple algorithm but requires a square or cubic grid. LSM represents a smooth interface but is prone to volume loss during calculations. VOF ensures no volume loss in the simulations but requires advanced algorithms, such as Piecewise Linear Interface Calculation, to maintain a sharp interface. Among these methods, VOF remains particularly popular for studying flows in microfluidic systems due to its simplicity and ease of implementation.

Although some previous studies have explored the effect of inserting obstacles into the microfluidic T-junction device (MFTD), none have investigated obstacles with the National Advisory Committee for Aeronautics (NACA) shape. This study investigates a semi-NACA-shaped squeezer using a two-dimensional numerical model based on the VOF method. We examine the effects of squeezer size, capillary number, and water fraction, and viscosity ratio on flow characteristics within the microfluidic system.

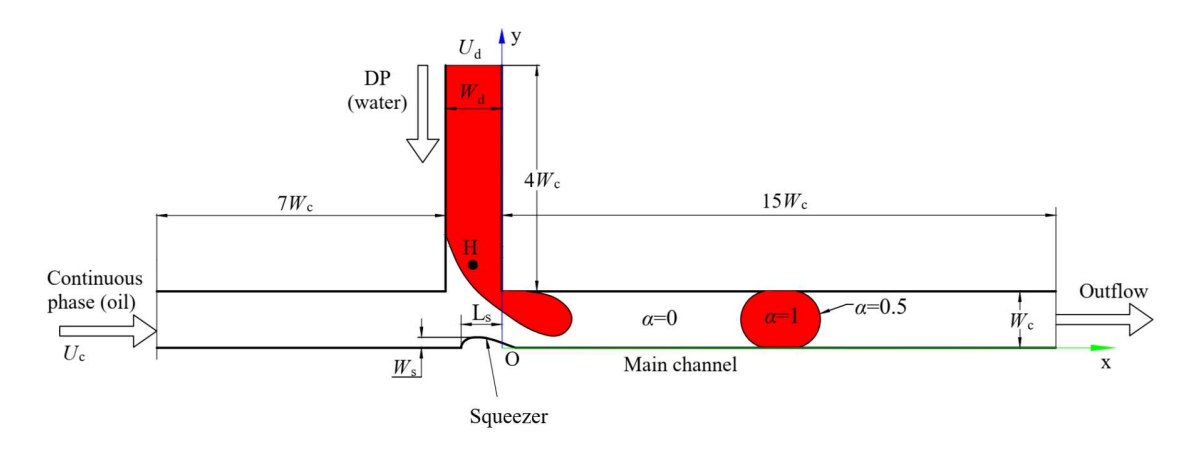


Fig. 1. Numerical model.

## 2. Numerical Methodology

A numerical model of the fabricated MFTD is illustrated in Fig. 1. In this figure,  $W_c$  represents the main channel width, which is used as the characteristic length. The other dimensions of the numerical model are also provided in Fig. 1. The novel design incorporates a semi-NACA-shaped squeezer into the main channel of the T-junction. This innovative approach aims to enhance our understanding of droplet dynamics within microfluidic systems. The precise placement of the squeezer is denoted by a distance  $L_s$ , measured along the x-direction from the origin O to the head of the squeezer. And  $W_s$  represents the thickness of the squeezer. H is the measurement point of pressure, which lies in the dispersed phase.

Due to the low Reynolds number, the flow in the channel remains laminar in most current microfluidic devices. Therefore, three fundamental equations are used to describe the fluid flow: the continuity equation, the Navier–Stokes equation, and the volume fraction equation, corresponding to Equations (1), (2) and (3) [21], respectively.

$$\tilde{\mathbf{N}} \times u = 0 \tag{1}$$

$$\rho\left(u_{t}+u\cdot\nabla u\right)=\nabla\cdot\left\{ -pI+\mu\left[\nabla u+\left(\nabla u\right)^{T}\right]\right\} +\sigma\kappa\delta n,\tag{2}$$

$$\alpha_{\rm f} + u \cdot \nabla \alpha = 0.$$
 (3)

In these equations, the values represent: p-pressure, u-velocity,  $\mu$ -bulk viscosity,  $\rho$ -bulk density. The subscript t represents the derivative with respect to time, while I denote the identity tensor. The final term of Eq. (2) represents the volumetric surface tension force, which acts exclusively at the interfaces between the fluid of the dispersed phase and the continuous phase. In this context,  $\sigma$ - the surface tension coefficient,  $\kappa$ - curvature, and n- unit normal vector of the interface are the corresponding quantities.  $\delta$  (the Dirac delta function) is nonzero only at the interface and zero elsewhere. This force is computed using the Continuum Surface Force (CSF) model introduced by Brackbill  $et\ al.\ [22]$ .

The model is non-dimensionalized, utilizing the primary channel width  $W_c$  as the characteristic length scale and the average velocity of the continuous phase  $U_c$  as the velocity scale. Consequently, the Reynolds number (Re) and the capillary number (Ca) are defined in Eq.  $(\ref{eq})$  [21]:

$$Re = \frac{\rho_c U_c W_c}{\mu_c}; Ca = \frac{\mu_c U_c}{\sigma}$$
 (4)

The density and the viscosity ratio are given in Eq. (5) [21]:

$$\gamma = \frac{\rho_d}{\rho_c}; \ \beta = \frac{\mu_d}{\mu_c} \tag{5}$$

A wall adhesion boundary condition is applied to modify the interface normal in cells adjacent to the wall, as described by Eq. (6) [21]:

$$\hat{n} = \hat{n}_{\rm w} \cos \theta_{\rm w} + \hat{t}_{\rm w} \sin \theta_{\rm w} \tag{6}$$

The unit vectors  $n_{\rm w}$  and  $t_{\rm w}$  correspond to the normal tangential directions, respectively. In this work, a fully non-wetting boundary condition is applied with  $\theta_{\rm w}$ =180°, ensuring that the dispersed flow does not adhere to the walls, resulting in well-shaped spherical droplets and predictable breakup behavior. A laminar, fully developed Poiseuille flow velocity profile, corresponding to the average inlet velocity, is applied to both inlets using a User-Defined Function (UDF). Water fraction (wf) represents the ratio of the dispersed phase flow rate to the total flow rate of the continuous and dispersed phases. In the dimensionless numerical model, the average velocity of dispersed flows was specified as  $U_d = wf/[\lambda(1-wf)]$  while  $U_c$  remains unity in all cases and  $\lambda = W_d/W_c$ . An atmospheric pressure condition is specified at the outlet to serve as the reference pressure for the system. To minimize the influence of the outlet boundary, it is positioned sufficiently far from the main junction. Within the investigated parameter ranges, this condition is satisfied by extending the channel length to fifteen times the width of the main branch. A no-slip condition is imposed on the channel walls.

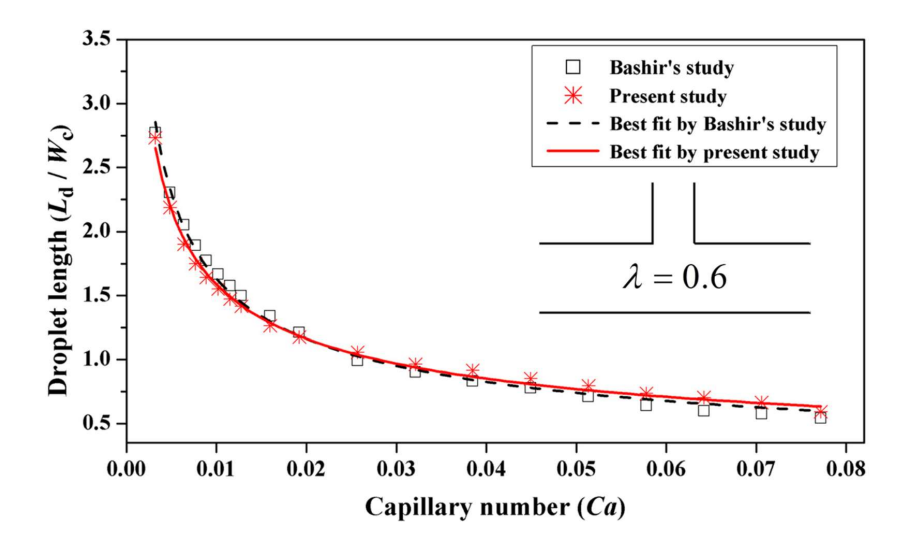


Fig. 2. Comparison between present result and the result obtained by Bashir's study [23].

To validate the accuracy of the numerical model, we compared the two-dimensional (2D) numerical simulation results for droplet length with the three-dimensional (3D) simulation results reported by Bashir *et al.* [23], shown in Fig. 2. Both cases show almost identical behavior of droplet length with respect to increasing capillary number [21]. While 3D effects significantly influence droplet formation and breakup in microfluidic T-junctions [24, 25], the 2D simulations conducted in this study still provide reliable qualitative insights into the flow behavior. Previous research has shown that when the aspect ratio of the channel (defined as the height over the main channel width,  $h/W_c$ ) falls below 0.05 [23], the impact of 3D phenomena becomes negligible, making 2D modeling a valid approximation under such geometric constraints. Thus, it can be demonstrated that the numerical model is well-suited for analyzing the droplet formation process and can be used for further studies.

#### 3. Results and Discussions

# 3.1. Effects of squeezer in the modified MFTD

Figure 3 illustrates the difference in droplet formation in a T-junction microfluidic system with and without a semi-NACA-shaped squeezer. In the channel without the squeezer, droplet formation follows the dripping regime. However, in the presence of the semi-NACA-shaped squeezer, the droplet formation transitions from the dripping to the squeezing regimes. This result indicates that the insertion of the semi-NACA squeezer alters the shear forces inside the channel. As the cross-sectional area narrows, the continuous phase locally accelerates, increasing the velocity within the squeezing region. The corresponding rise in the velocity increases leads to a sharp increase in the shear rate near the walls. Consequently, the faster continuous phase exerts a stronger pulling and pinching force on the dispersed phase, causing droplets to detach earlier and at smaller sizes. These findings further confirm the substantial influence of the squeezer on the flow dynamics within the channel.

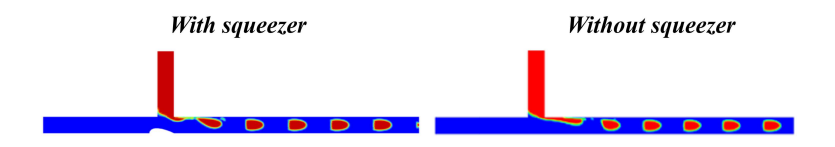


**Fig. 3.** T-junction microfluidic system with and without a semi-NACA shaped squeezer at Ca=0.3, wf=0.33.

# 3.2. The influence of capillary number on droplet formation regimes

To investigate the influence of capillary numbers on droplet formation regimes, three values of capillary number were examined: 0.1, 0.2, and 0.3. As shown in Fig. 4, the droplet formation regime transitions from squeezing to dripping as Ca increases from 0.1 to 0.2, and from dripping to jetting when Ca reaches 0.3. Simultaneously, droplet size decreases while the number of droplets increases with rising Ca. These findings align with previous studies, which suggest that a gradual increase in the capillary number leads to shifts in droplet formation regimes [22, 26].

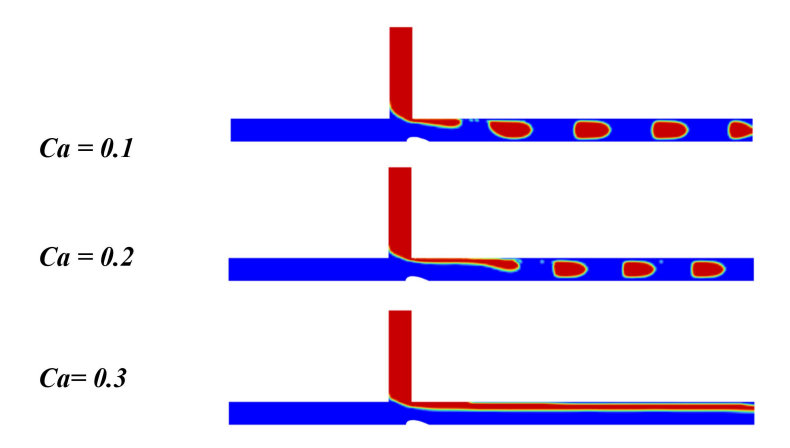
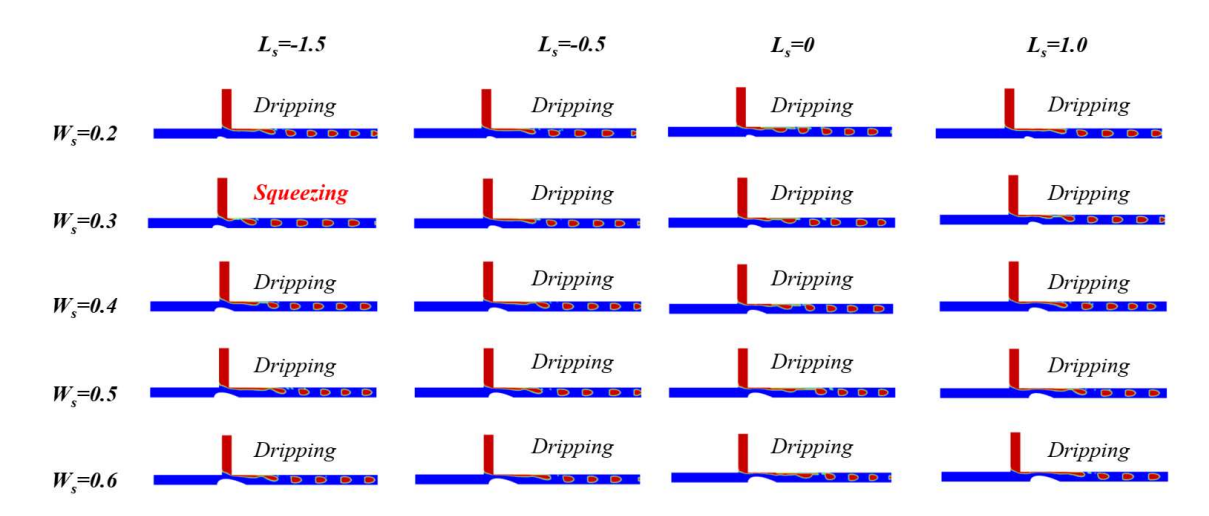


Fig. 4. Effect of Ca number on droplet formation in the channel at  $W_s$ =0.2, wf=0.4.

## 3.3. Effect of $W_s$ and $L_s$



**Fig. 5.** Effect of squeezer NACA shape thickness  $(W_s)$  and position  $(L_s)$  on droplet formation regime in the channel at Ca=0.3, wf=0.3.

To study the impact of the squeezer's size and position, we considered squeezer sizes within the range of  $W_s = \{0.2; 0.3; 0.4; 0.5; 0.6\}$  and four positions  $L_s = \{-1.5; -0.5; 0; 1.0\}$ . As shown in Fig. 5, two droplet formation regimes are observed in the channel: the squeezing and dripping regimes. When increasing  $L_s$  in the positive direction while keeping  $W_s$  constant, the droplet formation location shifts further away from the junction. This shift becomes more evident at higher  $W_s$  values. Similarly, when increasing  $W_s$  while keeping  $L_s$  constant, a comparable shift in the droplet formation position is observed. Notably, only when  $W_s = 0.3$  does the squeezing regime occur, whereas the dripping regime is observed in all other cases. This suggests that the dripping

regime predominantly forms due to high Ca conditions, where viscous forces are strong enough to stretch the dispersed-phase fluid. As a result, droplets are formed in the downstream regions of the junction (dripping regime) [11,27]. However, at  $L_s = -1.5$  and  $W_s = 0.3$ , the squeezing regime is observed. The droplet is created at the cross-junction position, which helps to create a more stable droplet with a more uniform droplet size. This configuration facilitates the generation of droplets closer to the junction at a high Ca value. Based on these findings, the optimal configuration for achieving the squeezing regime is a squeezer with  $W_s = 0.3$  and  $L_s = -1.5$ .

# 3.4. The influence of squeezer size on pressure and droplet size

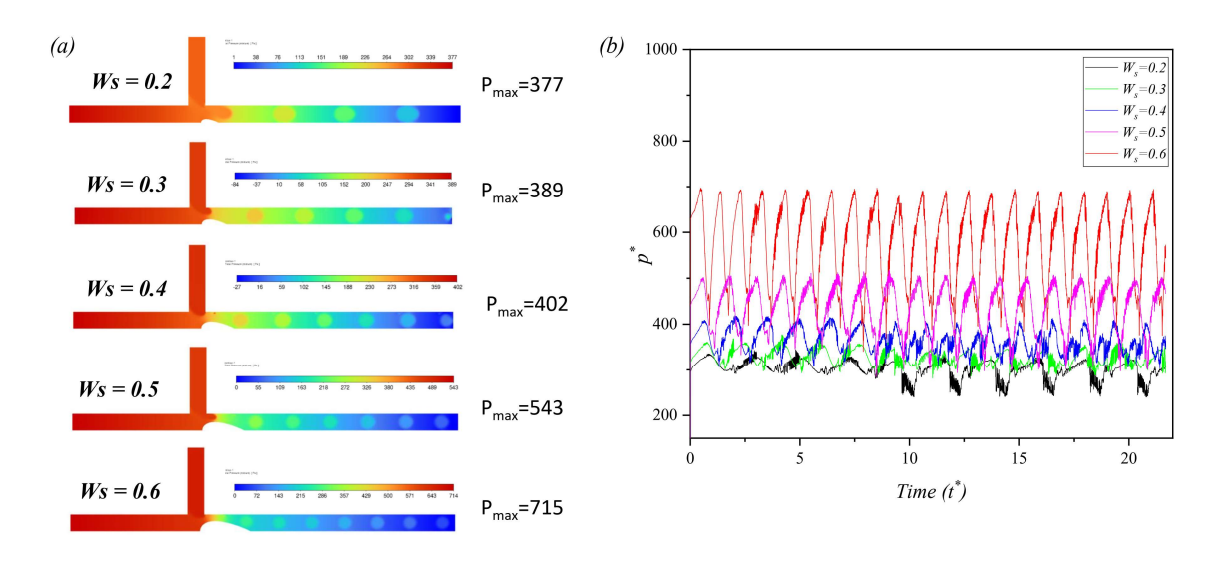


**Fig. 6.** (a) Qualitative and (b) Quantitative effect of  $W_s$  to pressure in the channel at Ca=0.05,  $L_s=-0.25$ , wf=0.3.

The squeezer size was varied from 0.2 to 0.6 to investigate its influence on pressure and droplet sizes. As shown in Fig. 6(a), as the squeezer size gradually increases, the pressure at both sides of the channel inlet also rises, expanding the overall pressure range. Specifically, at  $W_s$ =0.2, the maximum pressure is  $P_{max}$ =337, whereas at  $W_s$ =0.6, it reaches  $P_{max}$ =715. This indicates that as  $W_s$  increases, the pressure in front of the squeezer becomes significantly higher, creating favorable conditions for droplet detachment and size adjustment. The pressure diagram at point H (Fig. 6(b)) further confirms this trend, showing the highest pressure at  $W_s$ =0.6. Thus, under low Ca conditions, increasing the squeezer size raises the pressure at the channel entrance, facilitating droplet detachment.

Figure 7 presents the qualitative results of the squeezer size on droplet size. A clear increase in the number of droplets can be observed as  $W_s$  increases from 0.2 to 0.6. The increase in droplet quantity with larger  $W_s$  is due to the rise in pressure at the front of the channel, making droplet detachment easier (as shown in Fig. 7). At the same time, the droplet size decreased significantly when  $W_s$  were increased. The droplet diameter shows a rapid decline as  $W_s$  increases from 0.2 to 0.4, after which the reduction continues but at a slower rate.

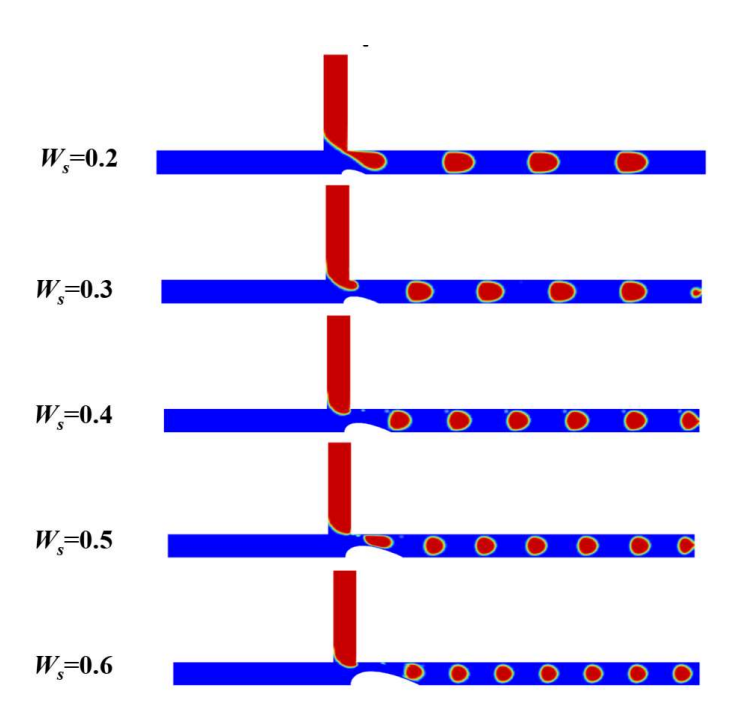


**Fig. 7.** Effect of  $W_s$  on droplet formation in the channel at Ca=0.05,  $L_s=-0.25$ , wf=0.3.

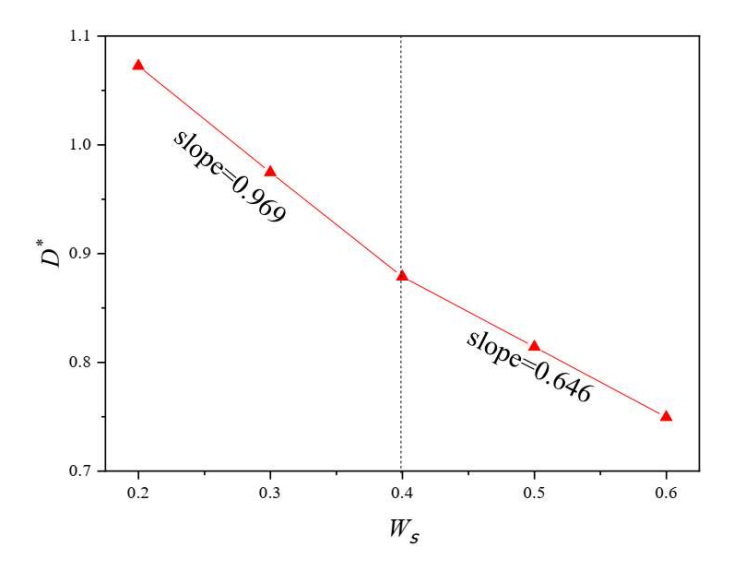


**Fig. 8.** Variation of droplet diameter in the channel at Ca=0.05,  $L_s=-0.25$ , wf=0.3.

Figure 8 presents the quantitative results of droplet diameter variation with  $W_s$ . The graph clearly shows a decrease in droplet diameter as  $W_s$  increases. Specifically, the droplet diameter

decreases rapidly when  $W_s$  increases from 0.2 to 0.4. Beyond  $W_s = 0.4$ , the droplet diameter continues to decrease but at a slower rate, as indicated by the change in the slope of the graph. These findings suggest that droplet size can be precisely controlled, enabling various applications in biomedical fields where tailored droplet sizes are essential for specific requirements.

# 3.5. The influence of viscosity on droplet formation

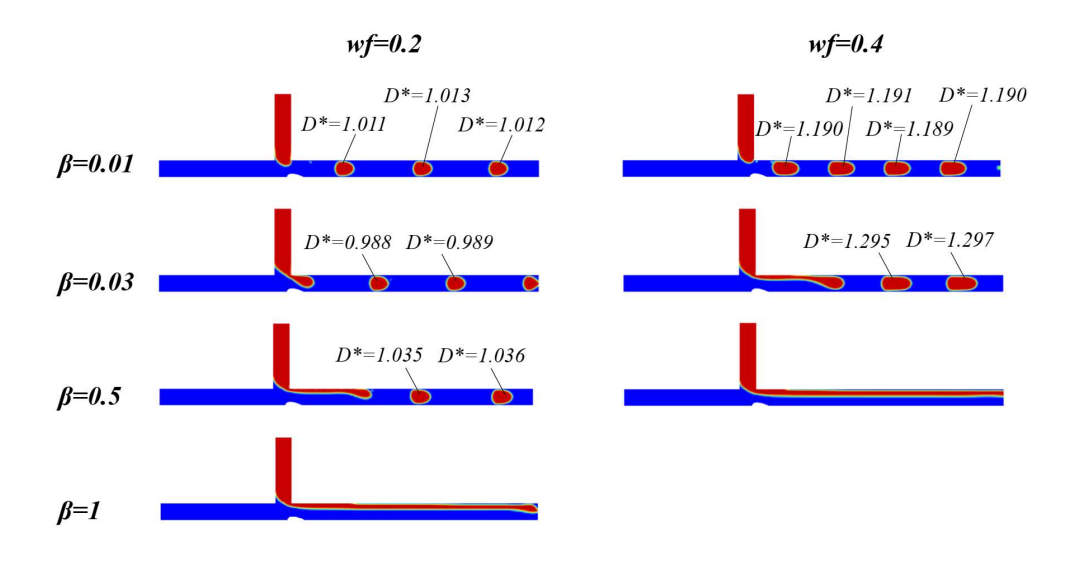


**Fig. 9.** Effect of viscosity at  $W_s$ =0.2,  $L_s$ =-0.25.

To investigate how the viscosity ratio between dispersed and continuous fluid flows affects droplet formation, a broad range of viscosity ratios (0.01 to 1.0) were studied while keeping other parameters constant. As shown in Fig. 9, transitions in flow regimes are observed, shifting from squeezing to jetting as the viscosity ratio increases. At lower viscosity ratios, droplet formation occurs in the squeezing regime due to the dominance of capillary forces. This phenomenon is attributed to the interaction between surface tension and viscosity in liquids. As the viscosity ratio decreases, the effects of surface tension become more dominant, as reported in previous studies [?]. Consequently, capillary forces play a crucial role in droplet formation when the viscosity ratio between the two fluids is low. At high viscosity ( $\beta = 1$ ), no droplets are formed, and the system remains in the jetting regime. This is because, at high  $\beta$ , capillary forces are weak, and the viscous forces dominate. This results in relatively weak interface shear stress, which facilitates the formation of a continuous liquid jet instead of discrete droplets. When the viscosity ratio decreases, the system transitions to the squeezing regime. In this regime, the droplet diameter size decreases as the viscosity ratio increases. Specifically, at wf = 0.2, the droplet diameter decreases from  $D^* = 1.011$  to  $D^* = 0.988$  as the viscosity ratio ( $\beta$ ) increases from 0.01 to 0.03. When transitioning from the squeezing to the squeezing-jetting regime, the droplet diameter gradually increases in both cases, with wf=0.2 and wf=0.4. Additionally, the droplet diameter increases when wf is raised from 0.2 to 0.4. These findings highlight the significant influence of the viscosity ratio on droplet formation within the channel.

### 4. Conclusion

In this study, a novel geometric design is proposed incorporating a semi-NACA-shaped squeezer into the main channel of a T-junction microfluidic system. The Volume of Fluid (VOF) method was employed to simulate droplet formation within the channel. The results indicate that the addition of the squeezer positively influences droplet formation. The study has demonstrated the influence of the capillary number on droplet formation: at low Ca, the squeezing regime is observed, whereas at high Ca, the dripping and jetting regimes dominate. Additionally, droplet size can be precisely controlled by adjusting the size and position of the semi-NACA-shaped squeezer. Furthermore, droplet formation is significantly affected by the viscosity ratio, with the squeezing regime transitioning into the jetting regime when the viscosity ratio exceeds 1. In the squeezing regime, droplet size decreases as the viscosity ratio increases. This novel design has promising applications in drug formulation, as it enables precise control over droplet size. Additionally, it can be integrated with advanced technologies to develop more complex microfluidic structures for research and industrial applications.

## Acknowledgements

This research is funded by Hanoi University of Science and Technology (HUST) under the project number T2023-PC-046.

#### **Conflict of interest**

The authors have no conflict of interest to declare.

#### References

- [1] M. T. Y. Yamaguchi, A. Kitagawa, Y. Ogawa, Y. Mizushima and R. Igarashi, *Insulin-loaded biodegradable PLGA microcapsules: initial burst release controlled by hydrophilic additives*, J. Control. Release, **81** (2002) 235.
- [2] Y. Liu and X. Jiang, Why microfluidics? Merits and trends in chemical synthesis, Lab. Chip. 17 (2017) 3960.
- [3] G. Muschiolik, Multiple emulsions for food use, Curr. Opin Colloid In. 12 (2007) 213.
- [4] X.-B. Li, F.-C. Li, J.-C. Yang, H. Kinoshita, M. Oishi, and M. Oshima, Study on the mechanism of droplet formation in T-junction microchannel, Chem. Eng. Sci., 69 (2012) 340.
- [5] S. Sohrabi, N. Kassir and M. Keshavarz Moraveji, Droplet microfluidics: fundamentals and its advanced applications, RSC Adv. 10 (2020) 27560.
- [6] a. F. G. a. R. D. Charles N. Baroud, Dynamics of microfluidic droplets, Lab. Chip, 10 (2010) 2032.
- [7] S. van Loo, S. Stoukatch, M. Kraft, and T. Gilet, *Droplet formation by squeezing in a microfluidic cross-junction*, Microfluid. Nanofluid. **20** (2016) 146.
- [8] A. Kovalev, A. Yagodnitsyna, G. Bartkus and A. Bilsky, *Control of plug flow dynamics in microfluidic T-junction using pulsations of dispersed phase flow rate*, Inter. J. Thermofluids **23** (2024) 100720.
- [9] Y. Zhang, J. Zhang, Z. Tang and Q. Wu, Regulation of gas-liquid Taylor flow by pulsating gas intake in micro-channel, Chem. Eng. J. 417 (2021) 129055.
- [10] I.-L. Ngo, S. Woo Joo, and C. Byon, Effects of Junction Angle and Viscosity Ratio on Droplet Formation in Microfluidic Cross-Junction, J. Fluids Eng. 138 (2016) 051202.
- [11] P. Garstecki, M. J. Fuerstman, H. A. Stone and G. M. Whitesides, Formation of droplets and bubbles in a microfluidic T-junction-scaling and mechanism of break-up, Lab. Chip. 6 (2006) 437.
- [12] K. Sripadaraja, M. N. Satyanarayan and G. Umesh, Generation of microdroplets in T-junction devices by pulsed fluid flow: Simulation studies, ISSS J. Micro. Smart Sys. 10 (2021), 103.
- [13] T. Thorsen, R. W. Roberts, F. H. Arnold and S. R. Quake, *Dynamic pattern formation in a vesicle-generating microfluidic device*, Phys. Rev. Lett. **86** (2001) 4163.

- [14] T. Nisisako, T. Torii and T. Higuchi, Droplet formation in a microchannel network, Lab. Chip. 2 (2002) 24.
- [15] G. F. Christopher, N. N. Noharuddin, J. A. Taylor, and S. L. Anna, Experimental observations of the squeezing-to-dripping transition in T-shaped microfluidic junctions, Phys. Rev. E 78 (2008) 036317.
- [16] W. Wang, Z. Liu, Y. Jin and Y. Cheng, LBM simulation of droplet formation in micro-channels, Chem. Eng. J. 173 (2011) 828.
- [17] A. J. Nath, D. K. Deka and S. Pati, Numerical Investigation of Droplet Generation Within a Microfluidic T-Junction With Semicylindrical Obstacle, J. Fluids Eng. 145 (2023) 011202.
- [18] H. Liu and Y. Zhang, Droplet formation in microfluidic cross-junctions, Phys. Fluids, 23 (2011) 082101.
- [19] W. Han, X. Chen, Z. Wu and Y. Zheng, *Three-dimensional numerical simulation of droplet formation in a microfluidic flow-focusing device*, J. Brazilian Soc. Mecha. Sci. Eng. **41** (2019) 1.
- [20] L. Sang, Y. Hong and F. Wang, *Investigation of viscosity effect on droplet formation in T-shaped microchannels by numerical and analytical methods*, Microfluid. Nanofluid. **6** (2008) 621.
- [21] I. L. Ngo, T. D. Dang, C. Byon and S. W. Joo, A numerical study on the dynamics of droplet formation in a microfluidic double T-junction, Biomicrofluid. 9 (2015) 024107.
- [22] D. B. K. J. U. Brackbill and C. Zemach, A Continuum Method for Modeling Surface Tension, J. Comput. Phys. 100 (1992) 335354.
- [23] S. Bashir, J. M. Rees and W. B. Zimmerman, Simulations of microfluidic droplet formation using the two-phase level set method, Chem. Eng. Sci. 66 (2011) 4733.
- [24] D. A. Hoang, L. M. Portela, C. R. Kleijn, M. T. Kreutzer and V. van Steijn, *Dynamics of droplet breakup in a T-junction*, J. Fluid Mech. **717** (2013) R4.
- [25] V. van Steijn, C. R. Kleijn and M. T. Kreutzer, Flows around confined bubbles and their importance in triggering pinch-off, Phys. Rev. Lett. 103 (20090 214501.
- [26] Y. Shi, G. H. Tang and H. H. Xia, Lattice Boltzmann simulation of droplet formation in T-junction and flow focusing devices, Comput. & Fluid. 90 (2014) 155.
- [27] P. G. M. De Menech, F. Jousse and H. A. Stone, Transition from squeezing to dripping in a microfluidic T-shaped junction. J. Fluid Mech., 595 (2008) 141.
- [28] H. A. S. Mads Jakob Jensen and Henrik Bruus, A numerical study of two-phase Stokes flow in an axisymmetric flow-focusing device, Phys. Fluid. 18 (2006) 077103.
- [29] Y. Yan, D. Guo and S. Z. Wen, Numerical simulation of junction point pressure during droplet formation in a microfluidic T-junction, Chem. Eng. Sci. 84 (2012) 591.